




Thermodynamic Investigation of the Hydrolysis Behavior of Fluorozirconate Complexes at 423.15–773.15 K and 100 MPa

Haibo Yan^{1,2} · Junjie He^{1,2} · Xiaowen Liu³ · Hongbo Wang³ · Junfeng Liu³ · Xing Ding⁴ 

Received: 14 August 2019 / Accepted: 25 March 2020 / Published online: 15 June 2020
© Springer Science+Business Media, LLC, part of Springer Nature 2020

Abstract

Metal complexes are thermally unstable in hydrothermal solutions, which may cause metal cation inertness or precipitation. We investigated, for the first time, the hydrolysis behavior of ammonium fluorozirconate ($(\text{NH}_4)_2\text{ZrF}_6$) at 423.15–773.15 K and 100 MPa. Kinetic equilibration experiments of the fluorozirconate solution demonstrated that the hydrolysis of the complex reached equilibrium within 4 h. Variable-temperature experiments showed that the complex's hydrolysis was dependent on the temperature and initial concentration in the hydrothermal solutions, with enhanced hydrolysis at elevated temperature and decreased initial concentrations. Based on our experimental data, we established a linear relationship between the cumulative hydrolysis constants (K) of $(\text{NH}_4)_2\text{ZrF}_6$ and absolute temperature T : $\ln K = (36.06 \pm 3.46) - (29747 \pm 1967)/T$, from which $\Delta_r H_m^\ominus$, $\Delta_r S_m^\ominus$ and $\Delta_r G_m^\ominus$ values for the hydrolysis reaction were also calculated. This study suggests that fluorine may play an important role in Zr mobility and provide a route to quantitatively characterize the thermodynamic features of metal complexes in hydrothermal solutions.

Keywords Zirconium · Hydrolysis behavior · Hydrothermal fluids · Mobility

1 Introduction

The chemical behavior of a metal element in aqueous solutions is mainly controlled by the nature of the metal ions or complex species that it forms [1]. It is well known that high-valence metal cations, cluster ions, and metal complexes can react with water molecules,

✉ Xing Ding
xding@gig.ac.cn; junfengliu@chd.edu.cn

¹ CAS Key Laboratory of Mineralogy and Metallogeny, Guangzhou Institute of Geochemistry, Chinese Academy of Sciences, Guangzhou 510640, China

² University of the Chinese Academy of Sciences, Beijing 100049, China

³ School of Earth Science and Resources, Chang'an University, Xi'an 710054, China

⁴ State Key Laboratory of Isotope Geochemistry, Guangzhou Institute of Geochemistry, Chinese Academy of Sciences, Guangzhou 510640, China

called hydrolysis, leading to the dissociation of water molecules and a change of the stability of the metal element [2, 3]. Therefore, these hydrolysis reactions play a significant role in the solubility and mobility of high-valence metal elements.

Zirconium (Zr) is an important rare metal element and has applications in the aerospace and defence industries, nuclear reactions, and atomic energy because of its physical and chemical properties, including excellent corrosion resistance, high melting point, high hardness, and strength. Zr can dissolve in hydrochloric and sulfuric acid, especially when fluorine is present, which greatly limits the utility of Zr metal [4]. A few studies have demonstrated that Zr has good stability and can form Zr–F complexes in F rich fluids [5–8]. The crystalline structures and calorimetric changes of these Zr–F complexes at different temperatures were also measured [9–11]; however, the thermodynamic properties of these Zr–F complexes in aqueous solutions, especially at high temperature and pressure, are still poorly understood. This makes it difficult to quantitatively study Zr solubility and mobility in solutions.

In this paper, we have adopted a pyrohydrolysis method to study the hydrolysis behavior of ammonium fluorozirconate ($(\text{NH}_4)_2\text{ZrF}_6$) in a hydrothermal solution, to determine its cumulative hydrolysis constants at 423.15–773.15 K and 100 MPa, with the aim of improving our understanding of the stability of the Zr–F complex in hydrothermal solutions.

2 Experimental and Analytical Methods

2.1 Chemicals

Fluorine is an essential inorganic ligand for Zr(IV) to form Zr–F ion complexes in aqueous solutions [12]. In this study, ammonium fluorozirconate ($(\text{NH}_4)_2\text{ZrF}_6$) (99%, AR, Xiya Reagent), a white powder with a density of $1.15 \text{ g}\cdot\text{cm}^{-3}$, was used as the starting material. This kind of Zr–F complex consists of a Zr–F octahedron and two N–H tetrahedrons (Fig. 1) [13, 14]. The Zr–F octahedron is composed of six fluorine atoms with a zirconium atom at its center, connected by covalent bonds. Through N–H covalent bonds, three hydrogens and one nitrogen form an N–H tetrahedron with the vertex nitrogen atom shared by four N–H tetrahedrons. The Zr–F octahedrons and N–H tetrahedrons are linked by weak ionic bonds, which can easily break to form two ionic groups. This complex's powder is highly soluble in water, forming a colorless solution at room temperature and ambient pressure.

2.2 Experimental Apparatus

All experiments were performed in Tuttle-type cold-seal pressure vessels of 27 mm outer diameter, 6 mm inner diameter, and 250 mm length, using water as a pressure medium in the hydrothermal laboratory at the Guangzhou Institute of Geochemistry [15]. This kind of pressure vessel is usually made of high-temperature nickel-base alloy, and consists of a longer vessel in which the open end and sealed parts are outside the furnace. In the vessels, the pressure is built up by the water through an external hydraulic pump and an air compressor, which produces an oxygen fugacity environment almost analogous to nickel–nickel oxide (NNO). The temperature was measured with a NiCr–Ni (K-type) thermocouple and was monitored by a high accuracy electronic temperature controller, while the pressure was corrected by high accuracy gauges. Temperature systematic error for the apparatus is $\pm 5 \text{ K}$, and pressure error is $\pm 10 \text{ MPa}$.

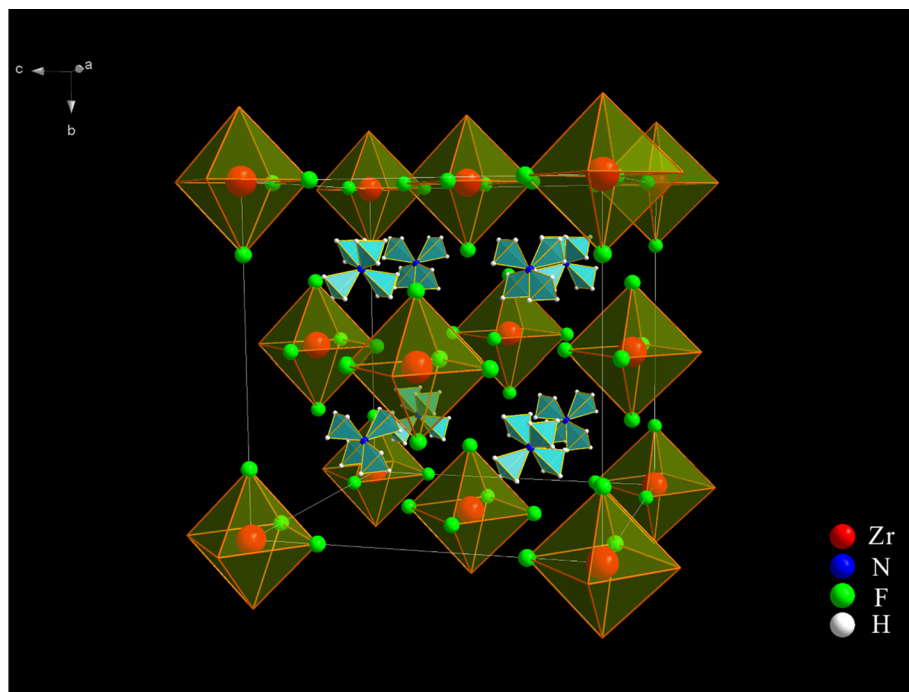


Fig. 1 The crystal structure of ammonium fluorozirconate ((NH₄)₂ZrF₆). The parameters of crystalline structure are described in the literature [13, 14]

2.3 Experimental Procedure

The hydrolysis experiments of (NH₄)₂ZrF₆ aqueous solutions were conducted with variable initial concentrations of 0.004, 0.005 and 0.01 mol·L⁻¹ at temperatures ranging from 423.15 to 773.15 K and a pressure of 100 MPa. By weighing with an analytical balance (± 0.1 mg, Sartorius, BS124S), 96.4 mg, 120.5 mg, and 241 mg (NH₄)₂ZrF₆ powder were dissolved into 100 mL deionized water to make ideal initial solutions of 0.004, 0.005, and 0.01 mol·L⁻¹, respectively. Due to the weighing error of making the solutions and the purity error of used chemical, which should lead to an initial Zr concentration deviation, all the three initial solutions, as well as the resultant solutions, were carefully analyzed as seen below. The measured initial Zr concentrations of 351 or 321 ppm, 560 ppm, and 1120 ppm were used for thermodynamic calculations.

Gold capsules, with a diameter of 4 mm and a length of 20–25 mm, were used as the reactant container. First, the capsules were pretreated by acid cooking, cleaning with alcohol and deionized water, and then dried at 333.15 K in a drying oven (DGG-9070B) to ensure no impurities were included. The capsules were then filled with about 100 μ L of the initial solutions and sealed at both two ends with a tungsten inert gas welding system (PUK U3, Germany). Before and after all experiments, the system was checked for leaks by placing the capsules into a drying oven at 383.15 K for at least 2 h. Only capsules with negligible mass differences were used in the experiments.

Before running an experiment, the gold capsule was placed into the end of the pressure vessel, followed by a nickel filler rod of ~ 10 cm length, which effectively reduces the thermal convection of the pressure-medium. After the experiments, the vessels were quickly quenched in an ice–water mixture. The temperature dropped to below 373.15 K in several seconds. Previous studies have demonstrated that this kind of quick-quench technique can effectively avoid the obvious re-dissolution of precipitates derived from the pyrohydrolysis of Ti–F complexes [15, 16]. Therefore, the quenching effect in this study is negligible. Finally, the capsules were cleaned and weighed again to ensure that no breakage occurred during the experiments.

2.4 Analytical Methods

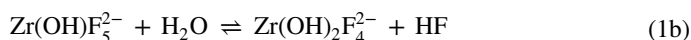
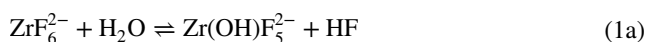
After the experiment, the product was processed carefully and analyzed accurately. The resultant solutions were extracted using a micropipette immediately after cutting open the capsules. Then the extracted aqueous solutions were centrifuged at 4500 rpm for 15 min, ensuring that the precipitates were separated from the solutions. The isolated solutions were removed by micropipette into 15 mL plastic containers and finally diluted with 3% nitric acid solution.

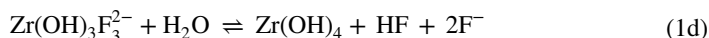
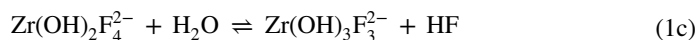
Zr concentrations of the initial and resultant solutions were measured using an iCAP Q ICP-MS (Thermo Fisher Scientific, USA) at the Analytical and Testing Center of Sun Yat-Sen University. The iCAP Q ICP-MS was equipped with a hydrofluoric acid-resistant sample introduction system, including a torch with sapphire inner tube, a micro Mist PFA nebulizer, and a Peltier cooled PFA Scott-type double pass spray chamber to avoid the interference of fluorine on the instrument and analytical results. All analyses were carried out with a plasma power of 1550 W, dwell time of 0.01 s, and sample depth of 5 mm. The Misa05-1, containing 1 ppm Zr determined at the State Key Laboratory of Isotope Geochemistry, Guangzhou Institute of Geochemistry, Chinese Academy of Sciences, was used as the external calibration standard solution for the mass discrimination correction of the mass spectrometer. Repeated tests of more than three times and the background deduction furthered the reliability of the results. The limit of detection for Zr is less than 0.1 ppt, and the accuracy of the analysis is greater than 3%.

3 Results and Discussion

3.1 Equilibrium of the Hydrolysis Reaction

Theoretically, ammonium fluorozirconate should hydrolyze at room temperature and atmospheric pressure. However, with increasing temperatures, the Zr–F complex should hydrolyze by a stepwise mechanism. A potential stepwise hydrolysis mechanism can be written as follows:





The reactions above occur as a nucleophilic substitution of an F^- in the Zr–F octahedron by a hydroxyl OH^- derived from the dissociation of H_2O [17]. This results in the formation of a series of Zr fluoro–hydroxyl complexes and Zr oxide precipitates corresponding to varying temperatures, pressures, and runtimes. At given conditions, once the hydrolysis reactions above reach equilibrium, the maximum Zr will precipitate from the reactive solutions to form Zr oxide. Consequently, the residual Zr concentrations in the reactive solutions remain constant no matter how the runtime changes.

Variable-time experiments with durations ranging from 2 to 12 h at 473.15 K and 100 MPa were conducted to determine the time required to reach equilibrium for the hydrolysis reaction. The residual Zr concentrations in the reactive solutions for each of the timed experiments are shown in Table 1. The experimental results show that the concentrations of residual Zr in the resultant solutions are 303 ppm, 270 ppm, 268 ppm, and 267 ppm at 473.15 K and 100 MPa at the run times of 2 h, 4 h, 8 h, and 12 h, respectively, with an initial Zr concentration of 351 ppm. This shows that concentrations of residual Zr decrease continuously for to 4 h and holds steady at around 270 ppm after 4 h, suggesting that the hydrolytic reaction has reached equilibrium at the fourth hour (Table 1 and Fig. 2). When the initial 321 ppm Zr solution was used as the starting material, the above reaction reached equilibrium within 2 h (Fig. 2). This implies that lower initial Zr concentrations in the reactive solutions will increase the Zr hydrolysis rate, and accelerate the hydrolysis reaction. In addition, elevated temperatures could also accelerate the rate of hydrolysis and shorten the required time to reach equilibrium for the hydrolysis of ZrF_6^{2-} [18]. This further implies that the exact equilibrium time of the hydrolysis reaction at temperatures

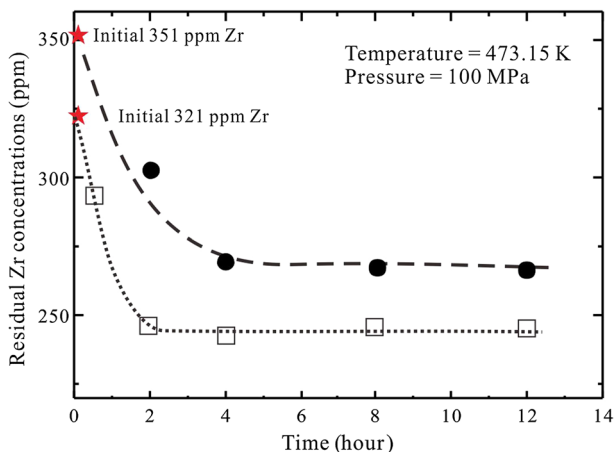
Table 1 Results of variable-time equilibrium experiments of $(\text{NH}_4)_2\text{ZrF}_6$ hydrolysis

Run no	Temperature ^a	Pressure ^b	Time	Initial Zr concentration	Residual Zr concentration
	(K)	(MPa)	(h)	(ppm)	(ppm)
Zr-2	473.15	100	2	351	303
Zr-3	473.15	100	4	351	270
Zr-4	473.15	100	8	351	268
Zr-5	473.15	100	12	351	267
18-Zr-011	473.15	100	0.5	321	283
18-Zr-012	473.15	100	2	321	244
18-Zr-006	473.15	100	4	321	239
18-Zr-010	473.15	100	8	321	244
18-Zr-013	473.15	100	12	321	243

^aThe temperature variations during the runs are less than 5 K

^bThe pressure variations are less than 10 MPa

Fig. 2 Residual Zr concentrations of $(\text{NH}_4)_2\text{ZrF}_6$ hydrolysis as a function of time during the kinetic equilibrium experiments. The dotted line represents the decreasing trend of residual Zr concentrations with increasing time

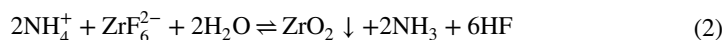


of more than 473.15 K is less than 4 h, while it is probably more than 4 h at temperatures of less than 473.15 K. Therefore, we carried out a series of experiments with a duration of 10–12 h, to ensure that the hydrolytic reaction would reach equilibrium.

The hydrolysis reactions of metal complexes reaches equilibrium more easily than the mineral dissolution. Similar to the Zr–F complex, other complexes, such as Sn–F and Ti–F complexes, can usually reach hydrolysis equilibrium within a dozen hours at temperatures ranging from 423.15 to 823.15 K and pressures of 50–400 MPa [16, 19]. However, mineral (e.g., ZrO_2) dissolution equilibrium took more time, up to several days [8]. This is most likely because the mineral dissolution, as well as consequent complexation, results from a series of more complex processes involving the solvation, hydrolysis, and nucleophilic substitution reactions on the solid–fluid interface [17]. Besides, controlled by the surface energy and specific surface of minerals, the dissolution rate of ZrO_2 minerals is much lower at hydrothermal conditions, leading to a longer equilibrium time.

3.2 Temperature and Initial Concentration Dependences of the Hydrolysis Reaction

Relative to ambient conditions, Zr–F complexes are less stable in the high temperature and high pressure conditions. In these experiments, initial solutions were hydrolyzed stepwise at a pressure of 100 MPa and temperatures ranging from 423.15 to 773.15 K. The cumulative hydrolysis reaction can be described as:



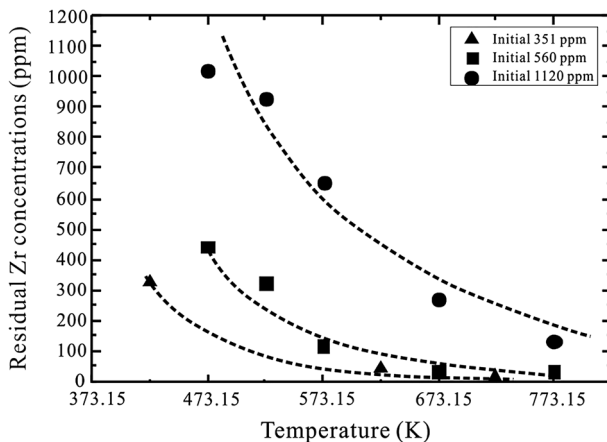
The residual Zr concentrations in the resultant solutions at temperatures ranging from 423.15 to 773.15 K and initial Zr concentrations varying from 351 to 1020 ppm are provided in Table 2 and Fig. 3. These data show that both initial Zr concentration and temperature can influence the stability of Zr–F complexes in F-rich solutions. As seen in Fig. 3, the residual Zr concentrations drop by one order of magnitude with increasing temperature despite different initial Zr concentrations. This suggests that elevated temperatures can promote the hydrolysis of $(\text{NH}_4)_2\text{ZrF}_6$ and lower the stability of Zr–F complexes in F-rich solutions, resulting in a negative effect.

Table 2 Results of $(\text{NH}_4)_2\text{ZrF}_6$ hydrolysis at varied temperatures and initial concentrations and the corresponding cumulative hydrolysis constants

Run no	Temperature/ K ^a	Pressure/ MPa ^b	Initial Zr/ ppm	Residual Zr/ ppm	$I/\text{mol}\cdot\text{L}^{-1}$	$c_{\text{HF}}/\text{mol}\cdot\text{L}^{-1}$	$c_{\text{NH}_4^+}/\text{mol}\cdot\text{L}^{-1}$	$c_{\text{ZrF}_6^{2-}}/\text{mol}\cdot\text{L}^{-1}$	$c_{\text{NH}_4^+}/\text{mol}\cdot\text{L}^{-1}$	$\gamma_{\text{ZrF}_6^{2-}}$	$\gamma_{\text{NH}_4^+}$	$\ln K$
Zr-9	423.15	100	351	323	0.0106	0.00185	0.000615	0.00355	0.00710	0.596	0.872	-36.23
Zr-10	623.15	100	351	42.9	0.00141	0.0203	0.00677	0.000471	0.000943	0.700	0.912	-11.24
Zr-11	723.15	100	351	7.32	0.000241	0.0227	0.00755	0.0000804	0.000161	0.792	0.943	-5.25
21	473.15	100	560	443	0.0146	0.00771	0.00257	0.00487	0.00974	0.513	0.837	-25.50
22	523.15	100	560	323	0.0106	0.0156	0.00521	0.00355	0.00710	0.515	0.838	-18.91
23	573.15	100	560	118	0.00389	0.0291	0.00971	0.00130	0.00259	0.614	0.881	-11.18
24	673.15	100	560	33.7	0.00111	0.0347	0.0116	0.000370	0.000741	0.681	0.906	-6.19
25	773.15	100	560	32.4	0.00107	0.0348	0.0116	0.000356	0.000712	0.538	0.853	-5.69
26	473.15	100	1120	1020	0.0336	0.00659	0.00220	0.0112	0.0224	0.394	0.774	-28.84
27	523.15	100	1120	929	0.0306	0.0126	0.0420	0.0102	0.0204	0.361	0.755	-23.25
28	573.15	100	1120	651	0.0215	0.0309	0.0103	0.00715	0.0143	0.363	0.758	-15.01
29	673.15	100	1120	267	0.00880	0.0562	0.0187	0.00293	0.00587	0.375	0.769	-7.61
30	773.15	100	1120	134	0.00442	0.0650	0.0217	0.00147	0.00295	0.305	0.730	-4.07

^aThe temperature variations during the runs are less than 5 K^bThe pressure variations are less than 10 MPa

Fig. 3 Experimental results of $(\text{NH}_4)_2\text{ZrF}_6$ hydrolysis at varied temperatures. The dotted lines represent the decreasing trend of residual Zr concentrations with increasing temperature in various initial Zr concentrations



Compared to the temperature, the initial Zr concentration shows a positive effect on the hydrolysis extent of Zr in F-rich solutions (Fig. 3). In solutions with an initial 351 ppm Zr concentration, with increasing temperatures ranging from 423.15 to 723.15 K, the residual Zr concentrations vary from 323 to 7.32 ppm (Table 2). In the initial 560 ppm Zr solutions, the residual Zr concentrations decrease from 443 to 32.4 ppm at temperatures of 473.15 to 773.15 K. Comparably, in the initial 1120 ppm Zr solutions, the residual Zr concentrations vary from 1020 to 134 ppm as the temperature increases from 473.15 to 773.15 K (Table 2). These further suggest that the higher Zr concentrations in the reactive solutions could decrease the hydrolysis rate of $(\text{NH}_4)_2\text{ZrF}_6$ and increase the stability of Zr–F complexes in hydrothermal solutions.

Similar temperature or initial concentration effects can also be seen in other experiments involving the complex hydrolysis or mineral dissolution [6, 8, 16, 19, 20]. The Ti–F complex is stable and hardly hydrolyzes at room temperature, but elevated temperatures can increase the hydrolysis rate and decrease the stability of the Ti–F complex, whereas high initial concentration is good for the stability of a complex [16]. A previous study found that the solubility of ZrO_2 can be increased with increasing temperatures in F-rich fluids [8]. Here is a paradox [17] that both Zr–F complex hydrolysis and ZrO_2 dissolution, which are reverse processes, are increased by the elevated temperatures. Although higher temperatures promote the hydrolysis of the Zr–F complex and lower the stability of Zr in F-rich solutions, it also facilitates the ZrO_2 dissolution and formation of the Zr–F complexes. Maybe high concentrations of the Zr–F complex in F-rich solutions played a major effect on the stability of Zr–F complex rather than the temperature. This should plausibly explain the paradox from the experimental results between the metal complex hydrolysis and mineral solubility.

3.3 Thermodynamic Properties During Hydrolysis

The extended Debye–Hückel equation [21, 22] was used to calculate the activity of ions in hydrothermal fluids in this experiment:

$$\log_{10}\gamma_i = -\frac{A_\gamma \cdot Z_i^2 \cdot \sqrt{I}}{1 + B_\gamma \cdot a \cdot \sqrt{I}} + b_\gamma I \quad (3)$$

where A_γ and B_γ are the parameters of the extended Debye–Hückel equation, and b_γ is the extended term parameter of NaCl, which can be used because the aqueous solution in this experiment can be simplified to a NaCl solution [8]. All the values of these three parameters (A_γ , B_γ , and b_γ) can be taken from the literature [8, 21, 23] (Table 3). The Z is the charge of the ion, and the subscript i represents the ion of interest. The a is the distance of closest approach. The distances of closest approach (a) were set at 2.5 Å for NH_4^+ [24] and 4.5 Å for Zr species, such as ZrF_6^{2-} [25]. I in Eq. 3 represents the ionic strength of the solution, which was calculated from Eq. 4:

$$I = \frac{1}{2} \sum_{i=1}^n c_i Z_i^2 \quad (4)$$

where c is the molarity of species, including NH_4^+ , HF, NH_3 , and Zr species such as ZrF_6^{2-} . Other species like H^+ and OH^- , were not considered because of their low concentrations in these experiments.

The equilibrium constant of the reaction 2 for $(\text{NH}_4)_2\text{ZrF}_6$ can be expressed as:

$$K = \frac{[\text{HF}]^6 [\text{NH}_3]^2}{[\text{NH}_4^+]^2 [\text{ZrF}_6^{2-}]} \quad (5)$$

When the activity coefficient (γ) is introduced into Eq. 5, it can be rewritten as:

$$K = \frac{c_{\text{HF}}^6 \gamma_{\text{HF}}^6 c_{\text{NH}_3}^2 \gamma_{\text{NH}_3}^2}{c_{\text{NH}_4^+}^2 \gamma_{\text{NH}_4^+}^2 c_{\text{ZrF}_6^{2-}} \gamma_{\text{ZrF}_6^{2-}}} \quad (6)$$

where the molarity of ZrF_6^{2-} was determined by the resultant products, and the molarities of HF, NH_3 , and NH_4^+ were determined by stoichiometric calculations based on the reaction 2, without considering the weak ionization of HF and NH_4^+ . The calculated results of the ionic strength, concentrations, and activity of ions, and cumulative hydrolysis constants

Table 3 The reference values of A_γ , B_γ , and b_γ at temperature of 423.15–773.15 K and pressure of 100 MPa described in the literature [20, 22]

Temperature (K)	Pressure (MPa)	A_γ ($\text{kg}^{1/2} \cdot \text{mol}^{-1/2}$)	B_γ ($\text{kg}^{1/2} \cdot \text{mol}^{-1/2} \cdot \text{cm}^{-1}$) $\times 10^{-8}$	b_γ ($\text{kg} \cdot \text{mol}^{-1}$) $\times 10^{-2}$
423.15	100	0.6352	0.3496	7.5
473.15	100	0.7196	0.3592	6.5
523.15	100	0.8192	0.3686	5.2
573.15	100	0.9398	0.378	3.5
623.15	100	1.0981	0.3882	1.1
673.15	100	1.3262	0.4004	−2.8
723.15	100	1.6723	0.4154	−9.3
773.15	100	2.1872	0.4321	−19.2

are shown in Table 2. The cumulative hydrolysis constant ($\ln K$) of $(\text{NH}_4)_2\text{ZrF}_6$ increases from -25.5 to -5.69 at temperatures ranging from 473.15 to 773.15 K with the initial 560 ppm Zr concentration, while it increases from -28.84 to -4.07 at the same temperature range but with an initial Zr concentration of 1120 ppm. These are similar to the solutions with an initial Zr concentration of 351 ppm, in which the cumulative hydrolysis constant changes from -36.23 to -5.25 as the temperature varies from 423.15 to 723.15 K (Table 2). Based on the above results, the cumulative hydrolysis constant of $(\text{NH}_4)_2\text{ZrF}_6$ has a positive correlation with temperature and is hardly affected by the initial Zr concentration. It further demonstrates that the equilibrium constant is a function of temperature, independent of the concentration.

Based on the Van't Hoff Equation (T , Kelvin)

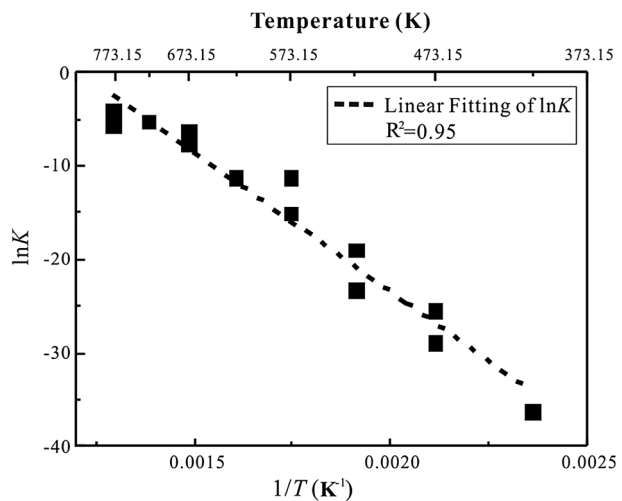
$$-\ln K = \frac{\Delta_r H_m^\ominus}{RT} - \frac{\Delta_r S_m^\ominus}{R} \quad (7)$$

and considering known the gas constant ($R=8.31451 \text{ J}\cdot\text{K}^{-1}\cdot\text{mol}^{-1}$) and the relationship between enthalpy, entropy, and temperature, there should be a linear relationship between $-\ln K$ and $1/T$. As shown in Fig. 4, the data were nicely fit with a line. The fitting equation is $\ln K = (36.06 \pm 3.46) - (29,747 \pm 1967)/T$ with $\Delta_r H_m^\ominus$ and $\Delta_r S_m^\ominus$ of reaction 2 calculated to be $(247.3 \pm 16.35) \text{ kJ}\cdot\text{mol}^{-1}$ and $(299.8 \pm 28.74) \text{ J}\cdot\text{mol}^{-1}\cdot\text{K}^{-1}$, respectively. As the temperature increases, the cumulative hydrolysis constant also increases, implying that the Zr–F complexes will be more unstable at elevated temperatures. Furthermore, a nice line fitting suitable to Eq. 7 testifies to the validity of the reaction 2 and the presence of ZrF_6^{2-} .

Significantly, a consistent result from the Zr–F, Ti–F, Nb–F, Ta–F, and Sn–F complexes in hydrothermal solutions is that the higher the temperature, the lower the residual metal concentration becomes [6, 16, 19, 20]. This will cause the residual metal concentration in the resultant solutions likely to be below the determination limits especially at temperatures over 873.15 K. Therefore, a linear relationship between $-\ln K$ and $1/T$ (Fig. 4) as described in this study will allow one to derive the cumulative hydrolysis constants not only at higher temperatures but at lower ones through an extrapolation method. This will also greatly promote the applications of the pyrohydrolysis results of metal complexes.

Given the Gibbs energy equation (T , Kelvin)

Fig. 4 Cumulative hydrolysis constants of $(\text{NH}_4)_2\text{ZrF}_6$ and their linear fitting based on the Debye–Hückel and van't Hoff equation



$$\Delta_r G_m^\ominus = \Delta_r H_m^\ominus - T \Delta_r S_m^\ominus \quad (8)$$

the change in the standard Gibbs energy ($\Delta_r G_m^\ominus$) of the hydrolysis reaction of the Zr–F complexes at different temperatures can be calculated and extrapolated to other temperatures. As shown in Table 4, $\Delta_r G_m^\ominus$ decreases from (150.42 ± 7.06) $\text{kJ}\cdot\text{mol}^{-1}$ to $-(74.43 \pm 14.49)$ $\text{kJ}\cdot\text{mol}^{-1}$ with the temperature changing from 323.15 to 1073.15 K, displaying a negative relationship between them. The data in this study suggest elevated temperatures promote the reaction 2 to happen spontaneously along the forward direction and facilitate the hydrolysis of Zr–F complexes.

3.4 The Mobility of Zirconium in Fluorine-Rich Fluids

The mobility of Zr is constrained by the temperature and initial concentration of the Zr–F complex. Elevated temperature can increase the velocity of molecules and ions and accelerate the reaction 2 in the forward direction, leading to a negative effect on the stability of Zr in F-rich solutions, similar to the stability of Zr in pure water and OH-rich solutions [8, 26, 27]. Many researchers have observed that the solubility of zircon is only 35 ± 11 ppm at 1203.15 K in pure water, and several ppm in the OH- and Cl-rich solutions [7, 28–32]. Hence, they hypothesized that Zr was highly unstable in the solutions and easily precipitated from the solutions. But other studies showed that the solubility of Zr in the F-rich fluids was orders of magnitude higher than in other aqueous systems and can reach thousands of ppm [7, 8], suggesting the enhanced Zr mobility in the F-rich solutions. When fluorine is enriched in an aqueous solution, the reaction 2 can shift in the opposite direction, resulting in more Zr dissolution in hydrothermal solutions. On the contrary, the reaction 2 goes in the forward direction when fluorine is absent or in low concentrations, which will significantly reduce the concentration of residual Zr in solutions. Therefore, at a given

Table 4 Calculated $\Delta_r G_m^\ominus$ and standard deviation at temperature of 323.15–1073.15 K based on Gibbs energy equation on the hydrolysis reaction of $(\text{NH}_4)_2\text{ZrF}_6$

Temperature (K)	$\Delta_r G_m^\ominus$ ($\text{kJ}\cdot\text{mol}^{-1}$)	Standard deviation ($\text{kJ}\cdot\text{mol}^{-1}$)
323.15	150.42	7.06
373.15	135.43	5.63
423.15	120.44	4.19
473.15	105.45	2.75
523.15	90.46	1.31
573.15	75.47	0.12
623.15	60.48	1.56
673.15	45.49	3.00
723.15	30.50	4.43
773.15	15.51	5.87
823.15	0.52	7.31
873.15	–14.47	8.74
923.15	–29.46	10.18
973.15	–44.45	11.62
1023.15	–59.44	13.06
1073.15	–74.43	14.49

temperature, fluoride concentrations in fluids play a crucial role in the Zr mobility and the stability of Zr–F complex.

4 Conclusions

Based on the high-temperature and high-pressure experiments, we found that the cumulative hydrolysis reactions between $(\text{NH}_4)_2\text{ZrF}_6$ and water at 423.15–773.15 K and 100 MPa can reach equilibrium within 4 h. This suggests that the complex's hydrolysis is much faster than mineral dissolution because of a homogeneous phase reaction. Variable-temperature experiments showed that higher temperatures and lower initial solution concentrations had a positive effect on the hydrolysis extent for $(\text{NH}_4)_2\text{ZrF}_6$. With the temperature increasing, the cumulative hydrolysis constants also increased. Using the Debye–Hückel and Van't Hoff equations, we fit the relationship between the cumulative hydrolysis constants (K) of $(\text{NH}_4)_2\text{ZrF}_6$ and temperatures (T , Kelvin) as the function:

$$\ln K = (36.06 \pm 3.46) - (29747 \pm 1967)/T,$$

where $\Delta_r H_m^\ominus$ and $\Delta_r S_m^\ominus$ are $(247.3 \pm 16.35) \text{ kJ}\cdot\text{mol}^{-1}$ and $(299.8 \pm 28.74) \text{ J}\cdot\text{mol}^{-1}\cdot\text{K}^{-1}$, respectively. The corresponding calculated $\Delta_r G_m^\ominus$ decrease from 150.42 to $-77.43 \text{ kJ}\cdot\text{mol}^{-1}$ as the temperatures ranges from 323.15 to 1073.15 K. These results imply that Zr–F complexes will be more unstable at elevated temperatures and that more fluorine could be required for the stability of Zr–F complexes in hydrothermal solutions.

Acknowledgements This study was supported by the National Key R&D Program of China (2016YFC0600204; 2016YFC0600408), the National Natural Science Foundation of China (41773054) and the CAS Science Innovation Project for College Students. This is contribution No. IS-2874 from GIGCAS. We thank LetPub (www.letpub.com) for its linguistic assistance during the preparation of this manuscript.

References

1. Baes, J.C.F., Mesmer, R.E.: The thermodynamics of cation hydrolysis. *Am. J. Sci.* **281**, 935–962 (1981)
2. Holovko, M., Druchok, M., Bryk, T.: Primitive model for cation hydrolysis: a molecular-dynamics study. *J Chem. Phys.* **123**, 154505 (2005)
3. Holovko, M., Druchok, M., Bryk, T.: Cation Hydrolysis Phenomenon in Aqueous Solution: Towards Understanding It by Computer Simulations. Springer, Berlin (2009)
4. Considine, G.D.: Zirconium. *Van Nostrand's Encyclopedia of Chemistry*. Wiley, New York (2005)
5. Gieré, R.: Zirconolite, allanite and hoegbomite in a marble skarn from the Bergell contact aureole: implications for mobility of Ti, Zr and REE. *Contrib. Mineral. Petrol.* **93**, 459–470 (1986)
6. Rubin, J.N., Henry, C.D., Price, J.G.: The mobility of zirconium and other “immobile” elements during hydrothermal alteration. *Chem. Geol.* **110**, 29–47 (1993)
7. Ryzhenko, B.N., Kovalenko, N.I., Prisyagina, N.I., Starshinova, N.P., Krupskaya, V.V.: Experimental determination of zirconium speciation in hydrothermal solutions. *Geochem. Int.* **46**, 328–339 (2008)
8. Migdisov, A.A., Williams-Jones, A.E., van Hinsberg, V., Salvi, S.: An experimental study of the solubility of baddeleyite (ZrO_2) in fluoride-bearing solutions at elevated temperature. *Geochim. Cosmochim. Acta* **75**, 7426–7434 (2011)
9. Hampson, G.C., Pauling, L.: The structure of ammonium heptafluozirconate and potassium heptafluozirconate and the configuration of the heptafluozirconate group. *J. Am. Chem. Soc.* **60**, 2702–2707 (1938)
10. Krylov, A.S., Krylova, S.N., Laptash, N.M., Vtyurin, A.N.: Raman scattering study of temperature induced phase transitions in crystalline ammonium heptafluozirconate, $(\text{NH}_4)_3\text{ZrF}_7$. *Vib. Spectrosc.* **62**, 258–263 (2012)

11. Nerád, I., Mikšíková, E., Kubíková, B.: Calorimetric investigation of tripotassium zirconate heptafluoride K_3ZrF_7 . *J. Mol. Liq.* **290**, 111191 (2019)
12. Griffith, W.P., Wickins, T.D.: Raman studies on species in aqueous solutions. Part II. Oxy-species of metals of Groups VIA, VA, and IVA. *J. Chem. Soc. A* **1967**, 675–679 (1967)
13. Zalkin, A., Eimerl, D., Velsko, S.P.: Diammonium hexafluorozirconate. *Acta Crystallogr. Sect. C* **44**, 2050–2051 (1988)
14. Bukvetskii, B.V., Gerasimenko, A.V., Davidovich, R.L.: Crystalline-structure of $NH_4ZrF_5 \cdot 0.75H_2O$ and $(NH_4)_2ZrF_6$ ammonium fluorozirconates. *Koord. Khim.* **17**, 35–43 (1991)
15. He, J.J., Ding, X., Wang, Y.R., Sun, W.D.: The effects of precipitation-aging-re-dissolution and pressure on hydrolysis of fluorine-rich titanium complexes in hydrothermal fluids and its geological implications. *Acta Petrol. Sin.* **31**, 1870–1878 (2015). **(in Chinese with English abstract)**
16. He, J.J., Ding, X., Wang, Y.R., Sun, W.D.: The effect of temperature and concentration on hydrolysis of fluorine-rich titanium complexes in hydrothermal fluids: Constraints on titanium mobility in deep geological processes. *Acta Petrol. Sin.* **31**, 802–810 (2015). **(in Chinese with English abstract)**
17. Ding, X., Harlov, D.E., Chen, B., Sun, W.D.: Fluids, metals, and mineral/ore deposits. *Geofluids* **2018**, 1–6 (2018)
18. Mo, J.X.: Impact on chemistry reaction speed, balance and conversion ratio of temperature. *Higher Educ. Forum* **5**, 161–164 (2004). **(In Chinese with English abstract)**
19. Wang, Y., Chou, I.M.: Characteristics of hydrolysis of the complex Na_2SnF_6 in hydrothermal solutions: an experimental study. *Chin. J. Geochem.* **6**, 372–382 (1987)
20. Wang, Y., Gu, F., Yuan, Z.: Partitioning and hydrolysis of Nb and Ta and their implications with regard to mineralization. *Chin. J. Geochem.* **12**, 84–91 (1993)
21. Helgeson, H.C., Kirkham, D.H., Flowers, G.C.: *Am. J. Sci.* **281**, 1249–1516 (1981)
22. Tanger, J.C., Helgeson, H.C.: Calculation of the thermodynamic and transport-properties of aqueous species at high-pressures and temperatures-revised equations of state for the standard partial molal properties of ions and electrolytes. *Am. J. Sci.* **288**, 18–98 (1988)
23. Helgeson, H.C., Kirkham, D.H.: Theoretical prediction of the thermodynamic behavior of aqueous electrolytes at high pressures and temperatures; II, Debye-Hückel parameters for activity coefficients and relative partial molal properties. *Am. J. Sci.* **274**, 1089–1198 (1974)
24. Garrels, R.M., Christ, C.L.: *Solutions, Minerals, and Equilibria*. Harper and Row, New York (1965)
25. Kielland, J.: Individual activity coefficients of ions in aqueous solutions. *J. Am. Chem. Soc.* **59**, 1675–1678 (1937)
26. Aja, S.U., Wood, S.A., Williams-Jones, A.E.: The aqueous geochemistry of Zr and the solubility of some Zr-bearing minerals. *Appl. Geochem.* **10**, 603–620 (1995)
27. Mysen, B.: An in situ experimental study of Zr^{4+} transport capacity of water-rich fluids in the temperature and pressure range of the deep crust and upper mantle. *Prog. Earth Planet. Sci.* **2**, 38 (2015)
28. Schmidt, C., Rickers, K., Wirth, R., Nasdala, L.: Low-temperature Zr mobility: An in-situ synchrotron-radiation XRF study of the effect of radiation damage in zircon on the element release in $H_2O + HCl + SiO_2$ fluids. *Am. Mineral.* **91**, 1211–1215 (2006)
29. Newton, R.C., Manning, C.E., Hanchar, J.M., Colasanti, C.V.: Free energy of formation of zircon based on solubility measurements at high temperature and pressure. *Am. Mineral.* **95**, 52–58 (2010)
30. Ayers, J.C., Zhang, L., Luo, Y., Peters, T.J.: Zircon solubility in alkaline aqueous fluids at upper crustal conditions. *Geochim. Cosmochim. Acta* **96**, 18–28 (2012)
31. Bernini, D., Audétat, A., Dolejš, D., Keppler, H.: Zircon solubility in aqueous fluids at high temperatures and pressures. *Geochim. Cosmochim. Acta* **119**, 178–187 (2013)
32. Shikina, N.D., Vasina, O.N., Gurova, E.V., Popova, E.S., Tagirov, B.R., Shazzo, Y.K., Khodakovskii, I.L.: Experimental study of $ZrO_2(c)$ solubility in water and aqueous perchloric acid solutions at 150 and 250 °C. *Geochem. Int.* **52**, 82–87 (2014)